Total Synthesis and Comparative Evaluation of Luzopeptin A−C and Quinoxapeptin A−C

Dale L. Boger,* Mark W. Ledeboer, Masaharu Kume, Mark Searcey, and Qing Jin

Contribution from the Department of Chemistry and The Skaggs Institute for Chemical Biology, The Scripps Research Institute, 10550 North Torrey Pines Road, La Jolla, California 92037

Received August 19, 1999

Abstract: Full details of the total syntheses of luzopeptin A−C and quinoxapeptin A−C, C_2-symmetric cyclic depsidecapeptides bearing two pendant heterocyclic chromophores, are disclosed and serve to establish the quinoxapeptin relative and absolute configuration. Key elements of the approach include the late-stage introduction of the chromophore and penultimate L-Htp acylation permitting the divergent synthesis of the luzopeptins, quinoxapeptins, and structural analogues from a common advanced intermediate. Symmetrical pentadepsipeptide coupling and macrocyclization of the 32-membered ring conducted at the single secondary amide site provided the common cyclic decadepsipeptide. The convergent preparation of the required pentadepsipeptide with installation of the labile ester in the final coupling was achieved under surprisingly effective racemization-free conditions. The quinoxapeptins were shown to bind to DNA by high-affinity bisintercalation analogous to sandramycin and the luzopeptins. Significant similarities in the DNA binding of sandramycin and luzopeptin A were observed, and these compounds proved distinguishable from the quinoxapeptins, indicating that the structural alterations in the chromophore impact the affinity and selectivity more than the changes in the decadepsipeptide. The luzopeptins proved to be more potent cytotoxic agents than the corresponding quinoxapeptin, but the quinoxapeptins proved to be more potent inhibitors of HIV-1 reverse transcriptase. In addition, a well-defined potency order was observed in the cytotoxic assays (A > B > C) in which the distinctions were extraordinarily large, with the removal of each L-Htp acyl substituent resulting in a 100−1000-fold reduction in potency. An equally well-defined but reverse potency order was observed in HIV-1 reverse transcriptase inhibition (C > B > A). Thus, the non-naturally occurring synthetic precursor **6** (quinoxapeptin C) was found to exhibit the most potent HIV-1 reverse transcriptase inhibition in the series and to lack a dose-limiting in vitro cytotoxic activity, making it the most attractive member of the series examined.

The luzopeptins (**1**−**3**) and quinoxapeptins (**4**−**6**) are closely related members of a growing class of naturally occurring C_2-symmetric cyclic decadepsipeptides which also include quinaldopeptin and sandramycin (**6**)[1−4] that bind to DNA by bisintercalation (Figure 1). The luzopeptins were first isolated from *Actinomadura luzonensis*,[5] and their structures were established through the single-crystal X-ray structure determination of luzopeptin A by Clardy[6] and recently confirmed by total synthesis.[7] In addition to their potent cytotoxic activity (A > B ≫ C) and antitumor activity,[5,8−10] the luzopeptins have been shown to inhibit HIV reverse transcriptase (C > B > A).[4,11] Quinoxapeptins A and B, which were isolated more recently from a norcardioform actinomycete of indeterminant morphology obtained from a bark disc of *Betula papyrifera*,[12] were first identified at Merck while screening for HIV reverse transcriptase (RT) inhibition. Both the luzopeptins and quinoxapeptins were shown to inhibit single and double mutants responsible for the emerging clinical resistance to RT inhibitors, and luzopeptin C was found to be capable of suppressing HIV replication in infected MT-4 cells at noncytotoxic concentrations.[11,12] At the time of their disclosure, only the two-dimensional structure of the quinoxapeptins had been established. Because of their close

(1) Toda, S.; Sugawara, K.; Nishiyama, Y.; Ohbayashi, M.; Ohkusa, N.; Yamamoto, H.; Konishi, M.; Oki, T. *J. Antibiot.* **1990**, *43*, 796.

(2) Matson, J. A.; Bush, J. A. *J. Antibiot.* **1989**, *42*, 1763. Matson, J. A.; Colson, K. L.; Belofsky, G. N.; Bleiberg, B. B. *J. Antibiot.* **1993**, *46*, 162.

(3) Total synthesis of sandramycin: Boger, D. L.; Chen, J.-H. *J. Am. Chem. Soc.* **1993**, *115*, 11624. Boger, D. L.; Chen, J.-H.; Saionz, K. W. *J. Am. Chem. Soc.* **1996**, *118*, 1629.

(4) Boger, D. L.; Chen, J.-H.; Saionz, K. W.; Jin, Q. *Bioorg. Med. Chem.* **1998**, *6*, 85. Boger, D. L.; Saionz, K. W. *Bioorg. Med. Chem.* **1999**, *7*, 315.

(5) Konishi, M.; Ohkuma, H.; Sakai, F.; Tsuno, T.; Koshiyama, H.; Naito, T.; Kawaguchi, H. *J. Antibiot.* **1981**, *34*, 148. Ohkuma, H.; Sakai, F.; Nishiyama, Y.; Ohbayashi, M.; Imanishi, H.; Konishi, M.; Miyaki, T.; Koshiyama, H.; Kawaguchi, H. *J. Antibiot.* **1980**, *33*, 1087. Tomita, K.; Hoshino, Y.; Sasahira, T.; Kawaguchi, H. *J. Antibiot.* **1980**, *33*, 1098.

(6) Arnold, E.; Clardy, J. *J. Am. Chem. Soc.* **1981**, *103*, 1243. Konishi, M.; Ohkuma, H.; Sakai, F.; Tsuno, T.; Koshiyama, H.; Naito, T.; Kawaguchi, H. *J. Am. Chem. Soc.* **1981**, *103*, 1241.

(7) Luzopeptins A−C: Boger, D. L.; Ledeboer, M. W.; Kume, M. *J. Am. Chem. Soc.* **1999**, *121*, 1098. Quinoxapeptins A−C: Boger, D. L.; Ledeboer, M. W.; Kume, M.; Jin, Q. *Angew. Chem., Int. Ed.* **1999**, *38*, 2424.

(8) Huang, C.-H.; Mong, S.; Crooke, S. T. *Biochemistry* **1980**, *19*, 5537. Huang, C.-H.; Prestayko, A. W.; Crooke, S. T. *Biochemistry* **1982**, *21*, 3704. Huang, C.-H.; Mirabelli, C. K.; Mong, S.; Crooke, S. T. *Cancer Res.* **1983**, *43*, 2718. Huang, C.-H.; Crooke, S. T. *Cancer Res.* **1985**, *45*, 3768.

(9) Rose, W. C.; Schurig, J. E.; Huftalen, J. B.; Bradner, W. T. *Cancer Res.* **1983**, *43*, 1504. Huang, C.-H.; Crooke, S. T. *Anti-Cancer Drug Des.* **1986**, *1*, 87.

(10) Boger, D. L.; Chen, J.-H. *Bioorg. Med. Chem. Lett.* **1997**, *7*, 919.

(11) Take, Y.; Inouye, Y.; Nakamura, S.; Allaudeen, H. S.; Kubo, A. *J. Antibiot.* **1989**, *42*, 107. Inouye, Y.; Take, Y.; Nakamura, S.; Nakashima, H.; Yamamoto, N.; Kawaguchi, H. *J. Antibiot.* **1987**, *40*, 100.

(12) Lingham, R. B.; Hsu, A. H. M.; O'Brien, J. A.; Sigmund, J. M.; Sanchez, M.; Gagliardi, M. M.; Heimbuch, B. K.; Genilloud, O.; Martin, I.; Diez, M. T.; Hirsch, C. F.; Zink, D. L.; Liesch, J. M.; Koch, G. E.; Gartner, S. E.; Garrity, G. M.; Tsou, N. N.; Salituro, G. M. *J. Antibiot.* **1996**, *49*, 253.

10.1021/ja993019e CCC: $18.00
Published on Web 11/24/1999

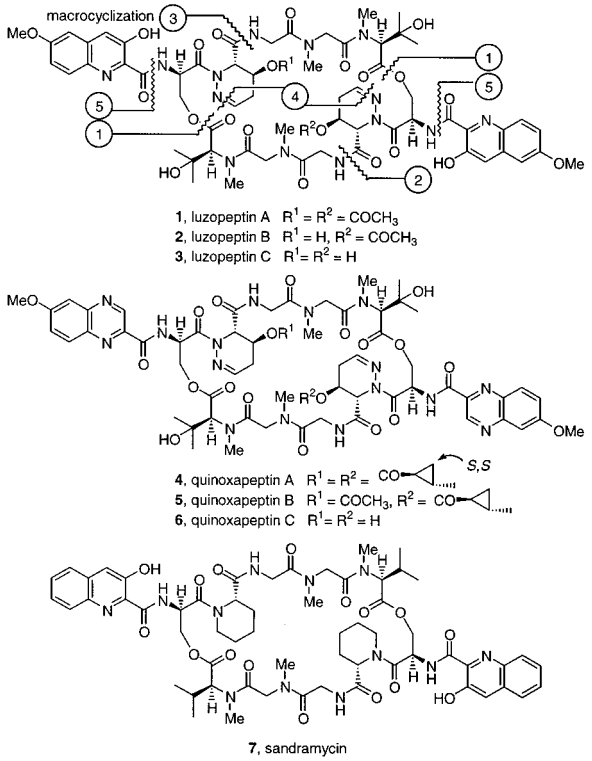

Figure 1. Structures of the luzopeptins, quinoxapeptins, and sandramycin.

structural relationship, the relative and absolute configuration of the quinoxapeptin cyclic decadepsipeptide could be safely assumed to be the same as those of the luzopeptins (established by X-ray), but that of the L-Htp acyl substituent was unknown. Thus, the total synthesis of the quinoxapeptins confirmed the relative and absolute configuration of the cyclic decadepsipeptide and established that of the 2-methylcyclopropanecarboxylic acid L-Htp acyl substituent.

Despite the potent biological activity of these natural products, there have been only a limited number of reported efforts toward the synthesis[13−16] of members of this family of DNA bisintercalators.[3,4,8,17−19] Herein, we provide the full details[7] of the total synthesis of luzopeptin A−C, quinoxapeptin A and B, and several key analogues from a common intermediate which unambiguously establish the relative and absolute stereochemistry of the quinoxapeptin acyl substituent, 2-methylcyclopropanecarboxylic acid, of the L-(4*S*)-hydroxy-2,3,4,5-tetrahydropyridazine-3-carboxylic acid (L-Htp) subunit. Since the luzopeptins and quinoxapeptins contain the identical cyclic decadepsipeptide core while differing only in the structure of the pendant chromophore and in the acyl substituent of the L-Htp subunit,

Scheme 1

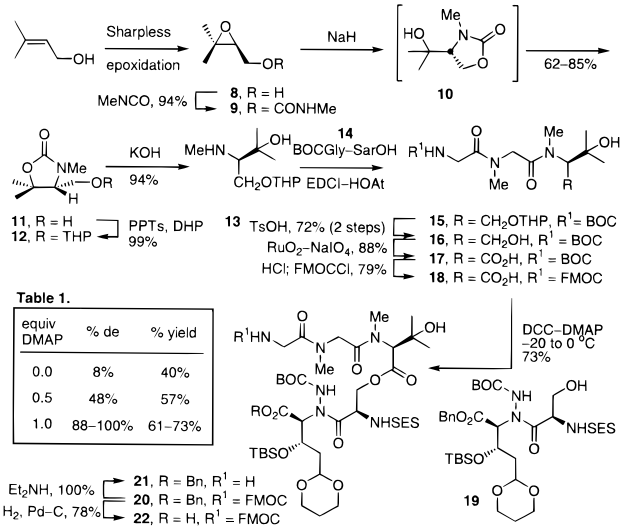

our strategy allows for a divergent synthesis of the luzopeptins, quinoxapeptins, and structural analogues from a common intermediate. Key elements of the synthesis include late-stage introduction of the chromophore and late-stage L-Htp acylation, symmetrical pentadepsipeptide coupling, and macrocyclization of the 32-membered decadepsipeptide conducted at the single secondary amide site. The convergent assemblage of the pentadepsipeptide with installment of the potentially labile ester linkage in the final coupling reaction is achieved surprisingly effectively under racemization-free conditions (Figure 1).

The quinoxapeptins were shown to bind to DNA by high-affinity bisintercalation analogous to sandramycin and the luzopeptins. Significant similarities in the DNA binding selectivity of sandramycin and luzopeptin A were observed, and these compounds proved distinguishable from the quinoxapeptins, indicating that the structural alterations in the chromophore impact the selectivity more than the changes in the decadepsipeptide.

Comparisons of the biological activities of the natural products and key analogues revealed important trends including the observation that **6**, which has not yet been identified as a natural product and was dubbed quinoxapeptin C in analogy with luzopeptin C, exhibits the most potent HIV-1 RT inhibition in the series and lacks a dose-limiting in vitro cytotoxic activity, making it the most attractive member of the series examined to date.

Pentadepsipeptide Synthesis. The *N*-methyl-β-hydroxyvalinol required for incorporation into the pentadepsipeptide **20** was prepared as summarized in Scheme 1. Sharpless epoxidation of 3-methyl-2-buten-l-ol with L-(+)-DIPT provided known (2*S*)-epoxide **8**.[20] Treament of **8** with methyl isocyanate gave the corresponding carbamate **9** (94%). Subsequent base-catalyzed epoxide opening generated **10**, which smoothly rearranged to the more stable cyclic carbamate **11** (>25:1) under the reaction conditions (5.0 equiv of NaH, THF, 25 °C, 24−72 h, 66−85%).[21] Protection of the primary alcohol as its THP ether (99%) was followed by hydrolysis of the carbamate (KOH, $(CH_2OH)_2$−H_2O, 150 °C, 25 h, 92−94%) to provide the desired amine **13**. Coupling of **13** with BOC-Gly-Sar-OH mediated by EDCI−HOAt[22] and subsequent acid-catalyzed removal of the

(13) Olsen, R. K.; Apparao, S.; Bhat, K. L. *J. Org. Chem.* **1986**, *51*, 3079.

(14) Hughes, P.; Clardy, J. *J. Org. Chem.* **1989**, *54*, 3260. Greck, C.; Bischoff, L.; Genet, J. P. *Tetrahedron: Asymmetry* **1995**, *6*, 1989.

(15) Ciufolini, M. A.; Swaminathan, S. *Tetrahedron Lett.* **1989**, *30*, 3027. Ciufolini, M. A.; Xi, *N. J. Chem. Soc., Chem. Commun.* **1994**, 1867. Xi, N.; Ciufolini, M. A. *Tetrahedron Lett.* **1995**, *36*, 6595. Ciufolini, M.; Xi, N. *J: Org. Chem.* **1997**, *62*, 2320. Xi, N.; Alemany, L. B.; Ciufolini, M. A. *J. Am. Chem. Soc.* **1998**, *120*, 80.

(16) Boger, D. L.; Schüle, *G. J. Org. Chem.* **1998**, *63*, 6421.

(17) Fox, K. R.; Davies, H.; Adams, G. R.; Portugal, J.; Waring, M. *J. Nucleic Acids Res.* **1988**, *16*, 2489. Fox, K. R.; Woolley, C. *Biochem. Pharmacol.* **1990**, *39*, 941.

(18) Searle, M. S.; Hall, J. G.; Wakelin, L. P. G. *Biochem. J.* **1988**, *256*, 271. Searle, M. S.; Hall, J. G.; Denny, W. A.; Wakelin, L. P. G. *Biochem. J.* **1989**, *259*, 433.

(19) Zhang, X.; Patel, D. J. *Biochemistry* **1991**, *30*, 4026. Leroy, J. L.; Gao, X.; Misra, V.; Gueron, M.; Patel, D. J. *Biochemistry* **1992**, *31*, 1407.

(20) Gao, Y.; Hanson, R. M.; Klunder, J. M.; Ko, S. Y.; Masamune, H.; Sharpless, K. B. *J. Am. Chem. Soc.* **1987**, *109*, 5765.

(21) Roush, W. R.; Adam, M. A. *J. Org. Chem.* **1985**, *50*, 3752. The crystallinity of **11** provided the opportunity to ensure pure material free of the isomer **10** was utilized.

THP group provided **16** (72% overall from **13**). Oxidation of the primary alcohol of **16** to the carboxylic acid was most reliably achieved with RuO_2-NaIO_4 (87%)[23] and was followed by BOC/FMOC exchange of the amine protecting group to provide **18** (79% from **17**).[24]

Esterification of **18** with the fully functionalized dipeptide **19**[16] incorporating an acyclic precursor to the L-Htp subunit was achieved with DCC−DMAP (3 equiv/2 equiv, CH_2Cl_2, −20 to 0 °C, 17 h, 73%)[3,7,25] in a surprisingly effective reaction. It was found that addition of increasing amounts of DMAP not only suppresses the racemization of the *N*-methyl-L-*β*-hydroxyvaline residue but also improves the overall reaction conversion (Table 1 in Scheme 1). Alternative coupling methods provided significantly lower conversions, and near complete racemization was observed when the reaction was run in the absence of DMAP.

To accurately quantify the extent of racemization, carboxylic acid **18** was prepared by an altenative route to ensure its enantiomeric purity. Thus, benzylation of **17** (2 equiv of BnBr, 1.2 equiv of $NaHCO_3$, DMF, 23 °C, 20 h, 84%) allowed for purificaton of the corresponding benzyl ester on a semipreparative Diacel Chiracel OD column in order to remove any minor enantiomer and provided *S*-**23** in enantiomerically pure form (eq 1).[26] Hydrogenolysis of *S*-**23** (10% Pd−C, CH_3OH, 23 °C,

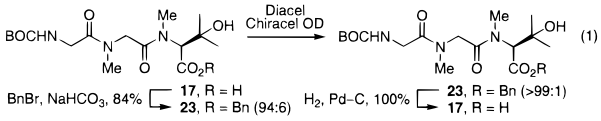

1 h, quantitative) regenerated **17** free from any contaminate enantiomer, which was converted to **18** as previously described. When this material was used in the esterification reaction, pentadepsipetide **20** was obtained as a single isomer without any detectable diastereomeric contaminants, thereby obviating the need for chiral chromatography purification, and diastereomerically pure material was used in the subsequent steps.[27]

With the **20** in hand, we examined the L-Htp ring-forming reaction which involves BOC deprotection, acetal cleavage, and imine cyclization (Scheme 2). Thus, treatment of **19** with TFA−H_2O (9/1, 23 °C, 2 h, 86%)[15,16] provided **24** in excellent yield and was accompanied by complete TBS deprotection. Likewise, **20** was smoothly converted to **25** under identical conditions (TFA−H_2O 9/1, 23 °C, 2.5 h, 68%). Importantly, both **24** and **25** proved stable to standard isolation, purification (SiO_2), and characterization techniques.

Scheme 2

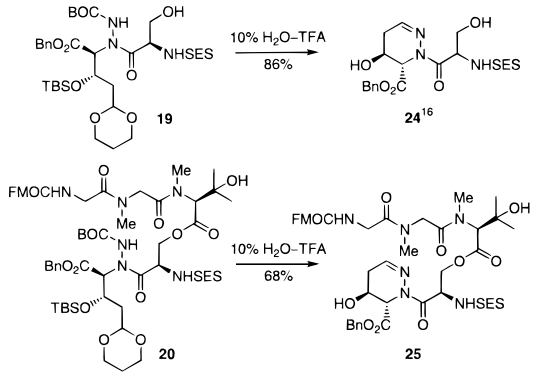

Scheme 3

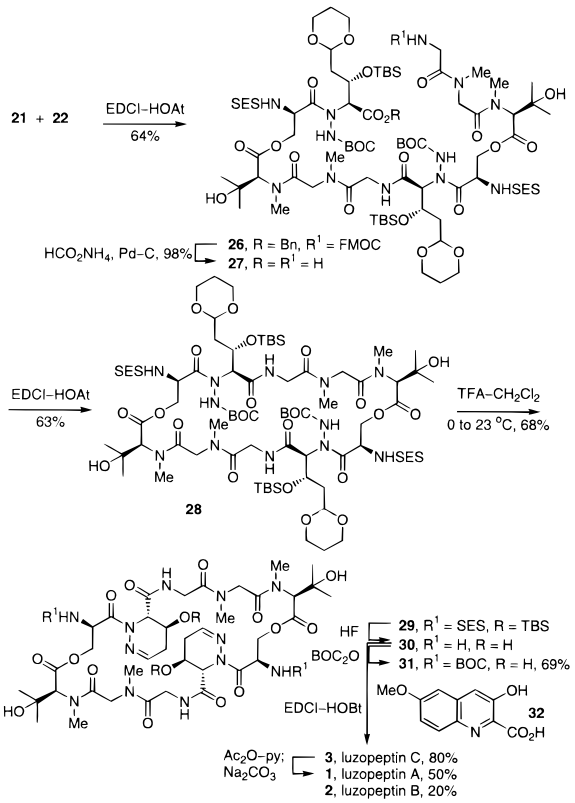

Cyclic Decadepsipeptide Formation and Completion of the Total Synthesis of Luzopeptin A−C. Linear decadepsipeptide formation was accomplished by independent deprotection of the amine and carboxylic acid of **20**. Selective removal of the benzyl ester of **20** (H_2, 10% Pd−C, 76−78%) conducted at 10−12 °C in order to minimize the slow but competitive loss of the FMOC protecting group provided **22**, while FMOC deprotection of **20** (Et_2NH-CH_3CN, ca. 100%) supplied the complementary coupling partner **21**. Coupling of **21** and **22** was mediated by EDCI−HOAt (CH_2Cl_2, 0 °C, 2 h, 64%), providing **26**, and proceeded smoothly in the absence of added bases (Scheme 3). Addition of bases (*i*-Pr_2NEt or *sym*-collidine) and the use of DMF as a solvent substantially lowered the overall conversion and may reflect the substrate and product sensitivity to *β*-elimination or retro-aldol reactions. The FMOC group and the benzyl ester were cleaved in a single operation by transfer hydrogenolysis (25% aqueous HCO_2NH_4, 10% Pd−C, EtOH−H_2O, 98%)[29] to give crude amino acid **27** which was im-

(22) EDCI = 1-(3-dimethylaminopropyl)-3-ethylcarbodiimide hydrochloride; HOAt = 1-hydroxy-7-azabenzotriazole; DCC = 1,3-dicyclohexylcarbodiimide; DMAP = 4-dimethylaminopyridine; HOBt = 1-hydoxybenzotriazole; SES = 2-(trimethylsilyl)ethylsulfonyl.

(23) Carlsen, P. H. J.; Katsuki, T.; Martin, V. S.; Sharpless, K. B. *J. Org. Chem.* **1981**, *46*, 3936. A related sequence enlisting $KMnO_4$ as the oxidant on a luzopeptin dipeptide has been reported[15] and failed to provide **17** in our preliminary efforts.

(24) Carpino, L. A.; Han, G. Y. *J. Org. Chem.* **1972**, *22*, 3404.

(25) Hassner, A.; Alexanian, V. *Tetrahedron Lett.* **1978**, *19*, 4475.

(26) Analysis of the starting ester revealed that **23** existed as a mixture (94:6) of enatiomers. The major (*S*)-enantiomer of **23** was chromatographically purified on a semipreparative Diacel Chiracel OD column (10 *μ*m, 2 × 25 cm, 15% *i*-PrOH−hexane, 7.0 mL/min flow rate). The relative ratio of enatiomers was determined on an analytical Chiracel OD column (10 *μ*m, 0.46 × 25 cm, 10% *i*-PrOH−hexane, 1.0 mL/min flow rate). The efluent was monitored at 235 nm, and the enantiomers eluted with a retention time of 9.98 (major *S*-**23**) and 11.48 min (minor *R*-**23**), respectively ($\alpha = 1.15$).

(27) The epimers of **20** were chromatographically separated, and their relative ratio was determined on a semipreparative Diacel Chiracel OD column (10 *μ*m, 2 × 25 cm, 50% *i*-PrOH−hexane, 7.0 mL/min flow rate). The effluent was monitored at 265 nm, and the diastereomers eluted with a retention time of 26.3 (**20**) and 32.3 min (*epi*-**20**), respectively ($\alpha = 1.23$).

(28) Characterization of these three products may be found in the Supporting Information.

mediately subjected to macrocyclization (EDCI−HOAt 5.0 equiv/5.5 equiv, CH_2Cl_2, 0 °C, 2 h, 63% overall from **23**), providing the 32-membered cyclic decadepsipeptide **28**. This closure was unusually good given the large ring size being formed, and alternative reagents including DPPA (0%) and HATU−HOAt (ca. 20%) were less effective at promoting the macrocyclization. The well-defined ^{1}H NMR spectrum indicated that **28** adopts a single symmetrical rigid solution conformation and that the material was free of contaminate diastereomers. Attempts at installing the two L-Htp units by treatment of **28** with TFA−H_2O mixtures met with limited success. While some of the desired diol (12−42%)[28] could be generated, its formation was accompanied by variable amounts of the mono-TBS product (10−28%)[28] and an elimination product (37−65%)[28] derived from the loss of one of the L-Htp hydroxyl groups. However, this could be avoided by running the reaction under anhydrous conditions. Thus, treatment of **28** with TFA−CH_2Cl_2 in the presence of anisole (1/1/0.4, 0 °C for 2 h, 0 to 23 °C, 1 h, 68%) cleanly provided the fully functionalized cyclic decadepsipeptide **29** incorporating the L-Htp subunits without competitive OTBS cleavage. The alternative order of first closing the L-Htp subunit and then conducting the macrocyclization was also briefly examined in order to establish whether this more conformationally restricted substrate might close more readily. Thus, simultaneous benzyl ester and FMOC deprotection of **26**, treatment of the resulting **27** with 10% H_2O−TFA to promote L-Htp ring closure, and subsequent macrocyclization effected by treatment with EDCI−HOAt provided a mixture of **29** and the corresponding mono OTBS derivative (ca. 1:1) in variable conversions (20−55%). Although this was not carefully examined, this did not appear to present any advantage over the approach detailed in Scheme 3.

Completion of the synthesis required SES deprotection followed by incorporation of the appropriate chromophore. Removal of the NSES group proved challenging, and treatment of **28** or **29** with Bu_4NF or CsF[30] under a variety of conditions ($\pm BOC_2O$)[3] led to deprotection of the OTBS groups without removal of the NSES. Under more forcing conditions, deprotection attempts led to substrate degradation, presumably as a result of the basic nature of the reagents. In our search for an alternative and acidic set of conditions for NSES cleavage, we found that *N*-SES-Phe-OCH_3 could be deprotected upon treatment with anhydrous HF (neat, 0 °C, 1 h, 65%), while 70% HF−pyridine complex (25% in THF, or neat, 0 to 23 °C) was ineffective (eq 2). Gratifyingly, exposure of **29** to anhydrous

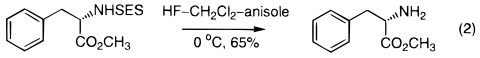

(2)

HF (neat, 2−3 mL, 100 μL of anisole/5−10 mg, 0 °C, 1−1.5 h) led to deprotection of both NSES and OTBS groups, providing **30** which could be converted to the corresponding NBOC derivative (**31**, 33, equiv of BOC_2O, 170 equiv of $NaHCO_3$, THF, 23 °C, 48 h, 69%) for identification purposes. Alternatively, coupling of **30** with 3-hydroxy-6-methoxyquinoline-2-carboxylic acid[31,32] (80% overall from **29**) without deliberate protection of the chromophore phenol provided luzopeptin C (**3**) identical in all respects (^{1}H NMR, ^{13}C NMR, IR, MS, $[\alpha]_D$) with natural material.[1,5] Peracetylation and subsequent mild basic hydrolysis of the phenolic acetates provided luzopeptin A (50%) and smaller amounts of luzopeptin B (20%) identical in all respects to natural material.[1,5,33]

Total Synthesis of Quinoxapeptin A−C and Establishment of the Absolute Stereochemistry. Since the absolute stereochemistry of the L-Htp acyl substituent was unknown, completion of the total syhthesis of quinoxapeptin A required incorporation of quinoxaline chromophore **33** and subsequent acylation with both (*S*,*S*)-**34** and (*R*,*R*)-**34**.[34] Comparison of the spectroscopic data with those reported for authentic material would establish the absolute stereochemistry. Thus, treatment of **29** with anhydrous HF provided **30** which was immediately coupled with 6-methoxyquinoxaline-2-carboxylic acid (**33**)[35] to provide **6** (65% overall from **29**), which was named quinoxapeptin C in analogy with the luzopeptins (Scheme 4). Quinoxapeptin C (**6**) was acylated with (*S*,*S*)-**34** (80%) and (*R*,*R*)-**34** (74%), providing **4** and **35**, respectively. From each of the acylation reactions a small amount of the mono-acylated product **36** (18%) or **37** (16%) was isolated. Comparison of the spectroscopic data established that **4** derived from (*S*,*S*)-**34** was identical to the spectroscopic data for quinoxapeptin A[12] and could be distinguished from **35** derived from (*R*,*R*)-**34**. Although the ^{1}H NMR spectra of **4** and **35** were nearly identical, the assignment rested on the distinguishable chemical shifts of the cyclopropane (δ 0.94/0.62 versus 0.87/0.72) and the Gly α-protons (δ 4.02 versus 3.98). The rigid conformation of the cyclic decadepsipeptide places the L-Htp acyl substituent above the Gly α-center, thereby perturbing the chemical shift of the cyclopropane protons and of one of the two Gly α-protons. In addition, chemical shifts for the Ser/Gly amide protons were also found to differ slightly (δ 9.00/8.95 versus 8.97/8.86). Acetylation of **36**, bearing the (*S*,*S*)-2-methylcyclopropanecarboxylic acid substituent, with Ac_2O (62%) provided quinoxapeptin B (**5**) which was identical to the natural material,[12] confirming the absolute stereochemistry assignment of the cyclic decadepsipeptide and the L-Htp acyl substituent. The bisacetate **38** was also prepared by acetylation of **6** (Ac_2O, 84%) to provide a direct comparison analogue to luzopeptin A differing only in the chromophore, and it may constitute an as yet unidentified member of the quinoxapeptin family of natural products.

DNA Binding Studies. Structural studies of luzopeptin A[18,19] and sandramycin[3] have confirmed their bisintercalation interaction with duplex DNA spanning two base pairs and shown that it requires two amide bond trans-to-cis isomerizations to allow the chromophores to adopt the appropriate distance and parallel orientation for binding. Both have been shown to bind to DNA with extremely high affinities (10^7 M^{-1}), and their binding significantly retards the mobility of DNA under nondenaturing electrophoretic conditions. The high affinity of sandramycin and a series of synthetic analogues has been demonstrated by surface plasmon resonance studies to be derived from the stability of the adduct formed between the duplex and

(29) Anwer, M. K.; Spatola, A. F. *Synthesis* **1980**, 929.

(30) Weinreb, S. M.; Demko, D. M.; Lessen, T. A. *Tetrahedron Lett.* **1986**, *27*, 2099.

(31) Prepared from methyl 2-benzyloxy-6-methoxyquinoline-2-carboxylate[32] by sequential treatment with H_2, 10% Pd−C, EtOH, 23 °C, 3 h (97%) and LiOH, THF/CH_3OH/H_2O 3/1/1, 23 °C, 10 h (70%).

(32) Boger, D. L.; Chen, J.-H. *J. Org. Chem.* **1995**, *60*, 7369.

(33) Altering the length of time exposed to the hydrolysis conditions alters the relative amounts of **1**−**3** obtained.

(34) Arai, I.; Mori, A.; Yamamoto, H. *J. Am. Chem. Soc.* **1985**, *107*, 8254. Mori, A.; Arai, I.; Yamamoto, H. *Tetrahedron* **1986**, *42*, 6447. The acid chlorides were prepared from the corresponding carboxylic acids (0.9 equiv of $(COCl)_2$, catalytic DMF, CH_2Cl_2, 0 °C for 10−15 min, 25 °C for 1−2 h) and used directly. For the carboxylic acid precursor to 1*R*,2*R*-**34**: $[\alpha]^{23}_D$ −74.4 (*c* 0.29, EtOH), lit. $[\alpha]^{24}_D$ −71.9 (*c* 1.00, EtOH). For the carboxylic acid precursor to 1*S*,2*S*-**34**: $[\alpha]^{23}_D$ +75.6 (*c* 0.25, EtOH). The ^{13}C NMR of **4** and **5** proved diagnostic of a *trans*- versus *cis*-2-methylcyclopropanecarboxylic acid ester (δ 18 versus 12 for CH_3), limiting the possibilities to 1*R*,2*R*-**34** or 1*S*,2*S*-**34**.

(35) Dumaitre, B. A.; Dodic, N.; Daugan, A. C. M.; Pianetti, P. M. C. PCT Int. Appl. WO9401408; *Chem. Abstr.* **1995**, *122*, 31342e. A detailed procedure for the preparation of **33** is provided in the Supporting Information.

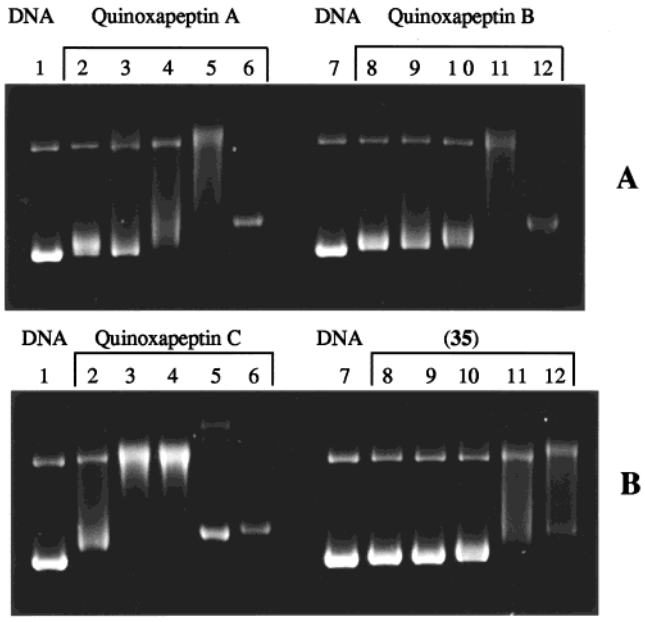

Figure 2. Agarose gel electrophoresis. (A) Lanes 1 and 7, untreated supercoiled ΦX174 DNA, 95% form I and 5% form II; lanes 2−6, quinoxapeptin A-treated ΦX174 DNA; lanes 8−12, quinoxapeptin B-treated ΦX174 DNA. The [agent]-to-[base pair] ratios were 0.022 (lanes 2 and 8), 0.033 (lanes 3 and 9), 0.044 (lanes 4 and 10), 0.11 (lanes 5 and 11), and 0.22 (lanes 6 and 12). (B) Lanes 1 and 7, untreated supercoiled ΦX174 DNA, 95% form I and 5% form II; lanes 2−6, quinoxapeptin C-treated ΦX174 DNA; lanes 8−12, *R,R*-quinoxapeptin A analogue (**35**)-treated ΦX174 DNA. The [agent]-to-[base pair] ratios were 0.022 (lane 2 and 8), 0.033 (lanes 3 and 9), 0.044 (lanes 4 and 10), 0.11 (lanes 5 and 11), and 0.22 (lanes 6 and 12).

the agent, with dissociation rate constants on the order of 10^{-5} s^{-1} ($t_{1/2}$ = 19 h).[4]

The sequence selectivity of sandramycin and a series of synthetic analogues has been studied by fluorescence and surface plasmon resonance binding studies. Using both techniques, sandramycin was shown to display a preference for 5′-purine−pyrimidine sequences, with the highest affinity for 5′-CATG. This sequence has a narrow minor groove and the lowest stability, and it allows the formation of H-bonds between two glycine amides (NH) and thymidine C2 carbonyls which were detected in the NMR-derived structures. However, the differences in sequence selectivity are relatively small, and attempts to footprint both the luzopeptins and sandramycin have met with limited success.[3,17] Details of the sequence selectivites of the luzopeptins remain unexplored, while studies of the DNA binding interactions of the quinoxapeptins have not been disclosed.

Bifunctional Intercalation. Confirmation that the luzopeptins and quinoxapeptins bind to DNA with intercalation was derived from their ability to induce the unwinding of negatively supercoiled DNA. This was established by their ability to gradually decrease the agarose gel electrophoresis mobility of supercoiled ΦX174 (unwinding) at increasing concentrations followed by a return to normal mobility (rewinding) at even higher agent concentrations. Similar types of changes have been reported for sandramycin[3] and luzopeptin A.[8] Under the conditions employed, both sandramycin and luzopeptin C completely unwound ΦX174 DNA at a 0.022 agent/base pair ratio (Figure 2 and Table 2), and quinoxapeptin C unwound ΦX174 DNA at a 0.033 agent/base pair ratio. Luzopeptins A and B and quinoxapeptins A and B completely unwound ΦX174 DNA at an even higher agent/base pair ratio, 0.044−0.011. Complete rewinding of the supercoiled DNA occurred at agent/base pair ratios of 0.044 for sandramycin, 0.044−0.11 for luzopeptin C and quinoxapeptin C, and 0.22 for luzopeptins A and B and quinoxapeptins A and B. These results suggest that sandramycin, luzopeptin C, and quinoxapeptin C bind to DNA with either a higher unwinding angle, a greater stability, or a slower off-rate than the other luzopeptins and quinoxapeptins, demonstrating that a small change in the structure has a significant effect on the DNA binding characteristics.

Table 2. Comparison of DNA Binding Properties

compound	K_B, M^{-1} (10^7)[a]	(−)-unwinding[b]	(+)-winding[c]
sandramycin	3.4 (10)	0.022	0.044
luzopeptin A	1.38 (5)	0.044−0.11	0.22
luzopeptin B		0.044−0.11	0.22
luzopeptin C		0.022	0.044−0.11
quinoxapeptin A	1.51 (4)	0.044−0.11	0.22
quinoxapeptin B	1.04 (4)	0.044−0.11	0.22
quinoxapeptin C	0.43 (3.5)	0.033	0.044−0.11
quin diacetate **38**		0.044−0.11	>0.22
37	0.22 (3.5)	0.044−0.11	>0.22
35		0.044−0.11	>0.22

[a] Apparent binding constant, calf thymus DNA. The base pair/agent ratio at saturated high-affinity binding is given in parentheses. [b] Agent/base pair ratio required to unwind negatively supercoiled ΦX174 DNA (form I to form II gel mobility, 1% agarose gel). [c] Agent/base pair ratio required to induce complete rewinding or postive supercoiling of ΦX174 DNA (form II to form I gel mobility, 1% agarose gel).

Further evidence of the effect of small perturbations in the depsipeptide structure on DNA binding is seen with quinoxapeptin diacetate **38**, the quinoxapeptin A monoester containing the *R,R*-stereochemistry in the cyclopropane ring (**37**), and the corresponding diester **35**. Each of these unnatural agents unwound ΦX174 DNA at agent/base pair ratios of 0.044−0.11 but failed to show any rewinding at agent/base pair ratios of 0.22. This suggests that the unnatural agents bind with a smaller unwinding angle, with lower stability, or with faster off-rates than the natural products.

DNA Binding Affinity. Apparent absolute binding constants and apparent binding site sizes were obtained by measurement of fluorescence quenching upon titration with calf thymus (CT) DNA. The excitation and emission spectra for the luzopeptins and the quinoxapeptins were determined in aqueous buffer (Tris-HCl, pH 7.4, 75 mM NaCl). The quinoxapeptins, which have the quinoxaline chromophore, exhibited intense fluorescence in solution with enhanced excitation (360 nm) and emission (460 nm) maxima when compared with the luzopeptins (excitation 340 nm, emission 520 nm) and sandramycin (excitation 360 nm, emission 530 nm) at similar concentrations. This greatly facilitated the measurement of fluorescence quenching in this series and allowed measurements to be carried out at initial agent concentrations of 1−10 μM. For the titration, small aliquots of CT-DNA (320 μM in base pairs) were added to 2 mL of a solution of the agent (10 μM) in Tris−HCl (pH 7.4), 75 mM NaCl buffer. Additions were carried out at 15-min intervals to allow equilibration. The titration was deconvoluted by Scatchard analysis using the equation $r_b/c = Kn - Kr_b$, where r_b is the number of agent molecules bound per DNA nucleotide phosphate, c is the free drug concentration, K is the apparent binding constant, and n is the number of agent binding sites per nucleotide phosphate. A plot of r_b/c versus r_b gives the association constant (slope) and the apparent binding site size (x-intercept) for the agents (see Table 2).

Analogous to previous studies, luzopeptin A[3] was found to exhibit a high affinity for duplex DNA (1.4×10^7 M^{-1}) with a saturating stoichiometry of 1:5 agent/base pairs, and this affinity is slightly less than that observed for sandramycin. Quinox-

Table 3. Comparative Oligonucleotide Binding Properties

		5′-GCATGC	5′-GCGCGC	5′-GCTAGC	5′-GCCGGC
sandramrnycin	K_B (10^7 M^{-1})	23.0	14.5	8.5	8.5
	$\Delta G°$ (kcal mol^{-1})	−11.4	−11.1	−10.8	−10.8
luzopeptin A	K_B (10^7 M^{-1})	28.4	12.7	10.3	14.3
	$\Delta G°$ (kcal mol^{-1})	−11.5	−11.0	−10.9	−11.1
quinoxapeptin A	K_B (10^7 M^{-1})	1.65	1.00	2.70	1.02
	$\Delta G°$ (kcal mol^{-1})	−9.8	−9.5	−10.1	−9.5
quinoxapeptin C	K_B (10^7 M^{-1})	1.12	0.68	1.95	1.00
	$\Delta G°$ (kcal mol^{-1})	−9.6	−9.3	−9.9	−9.5

apeptin A, constituting only a change of chromophore, has approximately the same affinity for duplex DNA as luzopeptin A. Removal of the cyclopropyl esters to generate quinoxapeptin B (minus one cyclopropyl ester) and quinoxapeptin C (minus both esters) causes an incremental decrease in affinity (A, 1.51×10^7 M^{-1}; B, 1.04×10^7 M^{-1}; C, 0.43×10^7 M^{-1}). This is in contrast to the luzopeptins, which have been demonstrated to increase in DNA binding affinity with removal of the acetate esters.[8] In our studies, solubility of luzopeptin B and C prevented confirmation of this result. The lower DNA binding affinity of quinoxapeptin C for duplex DNA, which was also consistently observed in the oligonucleotide studies (see below), suggests that the enhanced ability of this agent to unwind supercoiled DNA arises from something other than a greater binding affinity.

DNA Binding Selectivity. Preliminary studies of the DNA binding selectivity of luzopeptin A and quinoxapeptins A and C were conducted by measuring their absolute binding constants with the deoxynucleotides 5′-d(GCXXGC)$_2$, where XX = AT, GC, TA, and CG (Table 3). For each agent the characteristic fluorescence excitation and emission spectra were recorded in 10 mM Tris−HCl, 75 mM NaCl (pH 7.4) buffer. The addition of the deoxyoligonucleotides caused a marked quenching of fluorescence of the agents, with quenching ranging from 50 to 96%. To minimize fluorescence decrease due to dissolution or photobleaching, the solutions were stirred in 4-mL cuvettes in the dark with the minimum exposure to the excitation beam necessary to obtain a reading. The titrations were carried out with a 15-min equilibration time after deoxynucleotide addition. Scatchard plots of luzopeptin A binding to the deoxyoligonucleotides exhibited a downward convex curvature which, as in the case of sandramycin, we have interpreted to indicate a high-affinity bisintercalation and a lower affinity binding potentially involving monointercalation. Using the model described by Feldman[36] which assumes one ligand with two binding sites, we were able to deconvolute the curves according to the equation

$$r_b/c = {}^1/_2(K_1(n_1 - r_b) + K_2(n_2 - r_b) + \sqrt{(K_1(n_1 - r_b) - K_2(n_2 - r_b))^2 + 4K_1K_2n_1n_2}$$

where K_1 and K_2 represent the association constants for high- and low-affinity binding, and n_1 and n_2 represent the number of bound agents per duplex for the separate binding events. A typical plot for luzopeptin A is shown in Figure 3. Similar to sandramycin, luzopeptin A shows a marked affinity for 5′-GCATGC compared with the three other deoxyoligonucleotides. The distinctions are small but indicate a preference, like sandramycin, for the 5′-AT intercalation site. There is little, if any, discrimination by this agent for the other three sequences.

Quinoxapeptin A and quinoxapeptin C differed in their binding to the oligonucleotides. The Scatchard plots for both agents were only very slightly curved and approached linearity

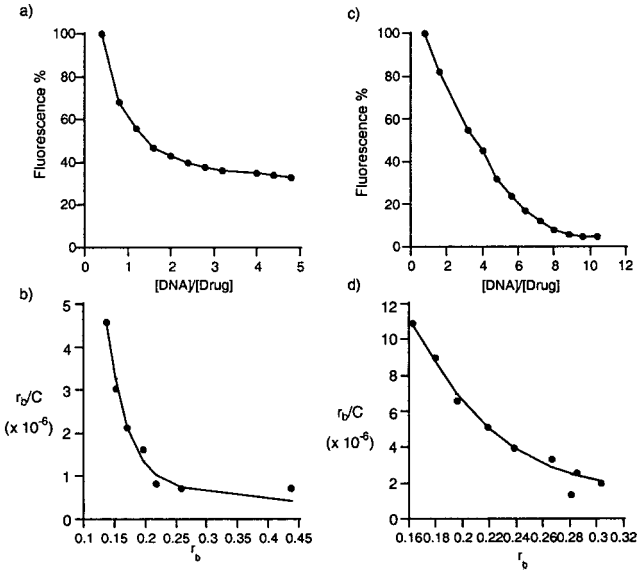

Figure 3. (a) Fluorescence quenching of luzopeptin A (excitation at 338 nm and emission at 530 nm in 10 mM Tris-HCl (pH 7.4) and 75 mM NaCl buffer solution) with increasing 5′-d(GCGCGC)$_2$ concentrations. (b) Scatchard plot of fluorescence quenching of luzopeptin A with 5′-d(GCGCGC)$_2$ (nonlinear fit). (c) Fluorescence quenching of quinoxapeptin A (excitation at 360 nm and emission at 460 nm in 10 mM Tris-HCl (pH 7.4) and 75 mM NaCl buffer solution) with increasing 5′-d(GCATGC)$_2$ concentrations. (d) Scatchard plot of fluorescence quenching of luzopeptin A with 5′-d(GCATGC)$_2$ (nonlinear fit).

such that both a linear, single-site analysis and a Feldman two-site analysis both gave almost identical values for the high-affinity binding constant. An example of the analysis using the latter approach is given in Figure 3. Interestingly, quinoxapeptin A has a significantly lower binding constant for the deoxyoligonucleotides than luzopeptin A. Comparisons between the binding constants of quinoxapeptin A and quinoxapeptin C remain qualitatively similar to those observed with duplex CT-DNA in that the latter compound consistently displays a lower DNA binding affinity than the former. Both were substantially less effective than luzopeptin A and sandramycin. In addition, the binding constants for quinoxapeptin A and C proved to be remarkably similar across the oligonucleotide series and, unlike those of luzopeptin A, showed a small preference for two of the sequences. Both agents bind with slightly higher affinity to 5′-AT (0.1−0.3 kcal mol^{-1}) and 5′-TA (0.5−0.7 kcal mol^{-1}), but the differences are relatively small. Notably, it is now the reverse 5′-TA vs 5′-AT that binds most tightly, and these differences stem from alterations in the chromophore.

Consequently, while there are substantial similarities in DNA binding properties of the agents in this class, bisintercalation spanning two base pairs, there are also significant differences in the stability, affinity, and selectivity of binding. These differences, which are derived from relatively small structural

(36) Feldman, H. A. *Anal. Biochem.* **1972**, *48*, 317.

Table 4. Biological Activity

	compound	HIV-1 RT[a] (μM)	L1210[b] (nM)	HCT116[c] (nM)
1	luzopeptin A	6	0.008	0.3
2	luzopeptin B	3	30	30
3	luzopeptin C	0.4	>100	>100
4	quinoxapeptin A	0.6	0.3	1
5	quinoxapeptin B	0.9	2	7
6	quinoxapeptin C	0.3	>100	>100
35		0.7	2	6
37		0.9	>100	>100
38		0.8	7	nd[d]
	sandramycin	2	0.001	0.007

[a] HIV-l reverse transcriptase inhibition. [b] L1210 mouse leukemia cytotoxic assay. [c] Human colon carcinoma assay. [d] Not determined.

changes, may account for the well-defined trends observed in their biological properties discussed below.

Biological Properties. The biological comparisons conducted with the synthetic samples are summarized in Table 4. The luzopeptins proved to be more potent cytotoxic agents than the corresponding quinoxapeptin, but the quinoxapeptins proved to be more potent inhibitors of HIV-1 reverse transcriptase. The quinoxapeptin derivative **35** possessing the unnatural (*R*,*R*)-2-methylcyclopropanecarboxylic acid substituent proved to be only slightly less potent than natural quinoxapeptin A (**4**) in both the HIV-RT and cytotoxic assays. In addition, the quinoxapeptins displayed activity trends analogous to those observed with the luzopeptins, with the important exception that the RT inhibition was more potent and the cytotoxic activity less potent, enhancing the selective RT inhibition observed with the quinoxapeptins. The comparison of the quinoxapeptin diacetate derivative **38** with luzopeptin A (**1**) is instructive in this regard, where **38** was nearly 10-fold more potent against HIV-1 RT and 1000 times less potent in the L1210 cytotoxic assay. The HIV-1 RT inhibition follows the trend of quinoxapeptin C > A analogous to the luzopeptin C > B > A potency, with the L-Htp-free alcohols being the most active agents in each series. The reverse potency order was observed in the cytotoxic assays with quinoxapeptin A ≫ C and luzopeptin A > B ≫ C, with the L-Htp-free alcohols being inactive. The distinctions here were extraordinarily large given the small structural differences with the removal of each L-Htp acyl substituent resulting in a 100-1000-fold reduction in potency. From comparisons that also include the more potent sandramycin (**7**) which lacks a comparable L-Htp substituent altogether, it appears as if substituents at this location diminish the cytotoxic potency and the presence of a free alcohol greatly reduces the potency. Thus, the synthetic precursor **6** (quinoxapeptin C), which has not yet been disclosed as a natural product, exhibits the most potent HIV-1 RT inhibition in the series and lacks a dose-limiting in vitro cytotoxic activity, making it the most attractive member of the series examined.

Experimental Section[37]

(2*S*)-1-[(*N*-Methylcarbamoyl)oxy]-3-methyl-2,3-epoxybutane (9). A solution of **8** (4.65 g, 45.5 mmol, 1 equiv) and Et_3N (12.6 mL, 91.0 mmol, 2 equiv) in CH_2Cl_2 at 25 °C was treated dropwise with methyl isocyanate (4.0 mL, 68.4 mmol, 1.5 equiv) and stirred for 2 h. The solution was quenched with H_2O (5 mL), poured into saturated aqueous NH_4Cl (50 mL), and extracted with CH_2Cl_2 (3 × 50 mL). The combined organic phase was dried ($MgSO_4$), filtered, and concentrated. Flash chromatography (SiO_2, 5% EtOAc−CH_2Cl_2) provided **9** (6.77 g, 42.6 mmol, 94%).

(37) Full characterization data are provided in the Supporting Information.

(4*R*)-4-(Hydroxymethyl)-3,5,5-trimethyl-2-oxazolidinone (11). A stirred suspension of NaH (2.24 g, 97.5 mmol, 5.9 equiv) in THF (40 mL) at 25 °C was treated dropwise with a solution of **9** (2.63 g, 16.5 mmol, 1 equiv) in THF (15 mL) and stirred for 36 h. The mixture was quenched dropwise with saturated aqueous NH_4Cl (20 mL) and extracted with CH_2Cl_2 (4 × 60 mL). The combined organic phases were dried ($NaSO_4$), filtered, and concentrated. Flash chromatography (SiO_2, 66% EtOAc−hexane) provided a mixture (>20:1) of isomers (1.63 g, 10.3 mmol, 62%, typically 62-85%) which was further purified by recrystallization (EtOAc−hexane).

(4*R*)-3,5,5-Trimethyl-4-1(tetrahydro-2*H*-pyran-2-yl)oxy]methyl]-2-oxazolidinone (12). A solution of **11** (4.40 g, 27.6 mmol, 1 equiv) and 3,4-dihydro-2*H*-pyran (3.3 mL, 36 mmol, 1.3 equiv) in CH_2Cl_2 (75 mL) at 25 °C was treated with pyridinium *p*-toluenesulfonate (PPTs, 350 mg, 1.39 mmol, 0.05 equiv) and stirred for 24 h. The solution was poured into half-saturated aqueous NaCl (100 mL) and extracted with CH_2Cl_2 (4 × 75 mL). The combined organic phase was dried ($MgSO_4$), filtered, and concentrated. Flash chromatography (SiO_2, 50% EtOAc−hexane) provided **12** (6.55 g, 27.0 mmol, 99%).

(2*R*,2′*RS*)-3-Methyl-2-(*N*-methylamino)-1-[(tetrahydro-2*H*-pyran-2′-yl)oxy]-3-butanol (13). A solution of **12** (6.50 g, 26.7 mmol, 1 equiv) and potassium hydroxide (7.50 g, 133 mmol, 5 equiv) in a mixture of ethylene glycol and H_2O (4:1, 55 mL) was warmed at reflux in a 150 °C bath for 20 h. The cooled solution was poured into half-saturated aqueous NaCl (100 mL) and extracted with CH_2Cl_2 (4 × 100 mL). The combined organic phase was dried ($MgSO_4$), filtered, and concentrated. Flash chromatography (SiO_2, 3% Et_3N−EtOAc) provided **13** (5.47 g, 25.1 mmol, 94%).

***N*-BOC-Gly-Sar-L-Me-Valinol(*β*-OH) (16).** A solution of BOCGly−SarOH (**14**, 562 mg, 2.28 mmol, 1.1 equiv), **13** (450 mg, 2.07 mmol, 1 equiv), and 2,6-lutidine (0.27 mL, 2.3 mmol, 1.1 equiv) in CH_2Cl_2−DMF (4:1, 10 mL) at 0 °C was sequentially treated with HOAt (310 mg, 2.28 mmol, 1.1 equiv) and EDCI (593 mg, 3.11 mmol, 1.5 equiv). The solution was stirred at 0 °C for 15 min, warmed to 25 °C, and stirred for an additional 24 h. The solution was diluted with CH_2Cl_2 (30 mL), washed with saturated aqueous $NaHCO_3$ (2 × 20 mL), 1 M aqueous HCl (2 × 20 mL), and saturated aqueous NaCl (1 × 50 mL), dried ($MgSO_4$), filtered, and concentrated to provide crude **15** (843 mg) which was used directly in the next reaction without purification. A solution of **15** (843 mg) in CH_3OH (4 mL) at 25 °C was treated with $TsOH{\cdot}H_2O$ (36 mg, 0.19 12 mmol, 0.1 equiv) and stirred for 2.5 h. The solution was concentrated, and flash chromatography (SiO_2, 5−10% CH_3OH−CH_2Cl_2 gradient) provided **16** (538 mg, 1.49 mmol, 72% overall from **13**).

***N*-BOC-Gly-Sar-L-Me-Val(*β*-OH)-OH (17). From 16.** A heterogeneous solution of **16** (3.30 g, 9.14 mmol, 1 equiv) in CCl_4−CH_3CN−H_2O (2:2:3, 92 mL) at 25 °C was treated with $NaIO_4$ (5.87 g, 27.4 mmol, 3 equiv) and $RuO_2{\cdot}H_2O$ (36 mg, 0.27 mmol, 0.03 equiv) and stirred for 24 h. The solution was poured into half-saturated aqueous $NaHCO_3$ (60 mL) and washed with CH_2Cl_2 (2 × 50 mL). The aqueous phase was diluted with EtOAc (50 mL) and acidified to pH 2 with concentrated HCl. The mixture was extracted with EtOAc (5 × 100 mL). The combined organic phase was dried ($MgSO_4$), filtered, and concentrated to provide **17** (3.00 g, 8.00 mmol, 88%).

From 23. A suspension of 23 (200 mg, 0.430 mmol) and 10% Pd−C (20 mg) in CH_3OH (20 mL) was stirred at 23 °C under H_2 for 1 h. Filtration and concentration in vacuo gave the acid *S*-**17** (176 mg, quantitative).

***N*-BOC-Gly-Sar-L-Me-Val(*β*-OH)-OBn (23).** A solution of **17** (3.00 g, 8.00 mmol) and BnBr (1.90 mL, 16.0 mmol) in DMF at 25 °C was treated with $NaHCO_3$ (806 mg, 9.60 mmol). After 20 h, the solution was poured into H_2O (100 mL) and extracted with EtOAc (5 × 100 mL). The combined organic phase was washed with saturated aqueous NaCl (100 mL), dried ($MgSO_4$), filtered, and concentrated. Flash chromatography (SiO_2, EtOAc) provided **23** (3.11 g, 6.69 mmol, 84%).

The major (*S*)-enantiomer of **23** was chromatographically separated on a semipreparative Diacel Chiracel OD column (10 μm, 2 × 25 cm, 15% *i*-PrOH−hexane; 7.0 mL/min flow rate). The relative ratio of enantiomers was determined on an analytical Chiracel OD column (10 μm, 0.46 × 25 cm, 10% *i*-PrOH−hexane, 1.0 mL/min flow rate). The effluent was monitored at 235 nm, and the enantiomers eluted with a

retention time of 9.98 (major *S*-**23**) and 11.48 min (minor *R*-**23**), respectively ($\alpha = 1.15$).

***N*-FMOC-Gly-Sar-L-Me-Val(*β*-OH)-OH (18).** A sample of **17** (90 mg, 0.24 mmol) was treated with 4.0 M HCl in dioxane (2.0 mL), and the solution was stirred at 25 °C for 30 min. The solution was concentrated to provide a yellow solid. The solid was stirred with anhydrous Et_2O for 2 min, and the solvent was removed in vacuo. This was repeated twice more. The solid was dissolved in 10% aqueous Na_2CO_3 (0.76 mL), cooled to 0 °C, and treated with a solution of FMOC-Cl (65 mg, 0.25 mmol, 1.05 equiv) in dioxane (0.65 mL). After 5 min, the solution was warmed to 25 °C and stirred for 8 h. The solution was poured into H_2O (10 mL) and washed with Et_2O (3 × 5 mL). The aqueous phase was acidified to pH 1 with concentrated HCl and extracted with $CHCl_3$ (5 × 10 mL). The combined organic phase was washed with saturated aqueous NaCl (10 mL), dried (Na_2SO_4), filtered, and concentrated to provide **18** (95 mg, 0.19 mmol, 79%).

Benzyl 2-[N^2-BOC-N^1-[*N*-SES-D-Ser(*N*-FMOC-Gly-Sar-L-Me-Val(*β*-OH))]-hydrazinol-3-(*tert*-butyldimethylsilyloxy)-4-(1,3-dioxan-2-yl)-(2*S*,3*S*)-butanoate (20). A solution of **18** (385 mg, 0.774 mmol) and **19** (300 mg, 0.387 mmol) in CH_2Cl_2 (2.3 mL) was dried over molecular sieves (4 Å) for 2 h. The solution was transferred to a reaction vessel, and CH_2Cl_2 (1.5 mL) was added. The solution was cooled to −25 °C, and DMAP (94.4 mg, 0.773 mmol) was added. After the complete dissolution of DMAP, DCC (1.16 mL, 1.0 M in CH_2Cl_2) was added. After 1 h, the reaction was warmed to 0 °C and stirred for 17 h. The reaction mixture was diluted with EtOAc (3.6 mL), the precipitate was removed by filtration, and the solution was concentrated. Flash chromatography (SiO_2, 75% EtOAc−hexane) provided a colorless foam (354 mg, 73%). The obtained product constituted a mixture of the desired compound **20** (major component, 88−100%) and the epimerized product *epi*-**20** (minor component, 0−12%).

The epimers of **20** were chromatographically separated, and their relative ratio was determined on a semipreparative Diacel Chiracel OD column (10 μm, 2 × 25 cm, 50% *i*-PrOH−hexane, 7.0 mL/min flow rate). The effluent was monitored at 265 nm, and the diastereomers eluted with a retention time of 26.3 (**20**) and 32.3 min (*epi*-**20**), respectively ($\alpha = 1.23$).

***N*-SES-D-Ser(*O*-(*N*-FMOC-Gly-Sar-L-Me-Val(*β*-OH)))-L-Htp-OBn (25).** A solution of **20** (8 mg, 4.32 limol) in 90% aqueous trifluoroacetic acid (0.5 mL) at 25 °C was stirred for 2.5 h. The solution was concentrated, diluted with EtOAc (10 mL), and washed with saturated aqueous $NaHCO_3$ (2 mL). The combined organic phase was dried ($MgSO_4$), filtered, and concentrated. PTLC (SiO_2, 10% CH_3OH−CH_2Cl_2) provided **25** (5.2 mg, 68%).

Benzyl 2-{N^2-BOC-*N*′-{*N*-SES-D-Ser[(2-(N^2-BOC-N^1-(*N*-SES-D-Ser-(*N*-FMOC-Gly-Sar-L-Me-Val(*β*-OH)))-hydrazino)-3-(*tert*-butyldimethylsilyloxy)-4-(1,3-dioxan-2-yl)-(2*S*,3*S*)-butanoyl)-Gly-Sar-L-Me-Val(*β*-OH)]}-hydrazino}-3-(*tert*-butyldimethylsilyloxy)-4-(1,3-dioxan-2-yl)-(2S,3S)-butanoate (26). A solution of **20** (60.0 mg, 47.8 μmol) in degassed CH_3OH (6 mL) at 10−12 °C was treated with 10% Pd−C (60 mg) and stirred under H_2 (balloon) for 3 h. The solution was filtered, and the solvents were removed in vacuo. The residue was dissolved in EtOAc (50 mL) and washed with 0.5% aqueous HCl (10 mL) and H_2O (10 mL), dried (Na_2SO_4), filtered, and concentrated to give crude acid **21** (42.3 mg) which was used directly in the next reaction without further purification.

A solution of **20** (45.0 mg, 35.8 μmol) in CH_3CN (0.6 mL) at 25 °C was treated with Et_2NH (0.3 mL) and stirred for 20 min. The solution was diluted with CH_3CN (2 mL) and the solvents were removed in vacuo to give **22** which was used directly in the next reaction without further purification.

A solution of acid **21**, amine **22**, EDCI (21.0 mg, 0.107 mmol), and HOAt (14.90 mg, 0.107 mmol) in CH_2Cl_2 (0.5 mL) at 0 °C was stirred for 2 h. The solution was concentrated, and the residue was dissolved in EtOAc (50 mL). The organic phase was washed with 2% aqueous HCl (10 mL), 1% aqueous $NaHCO_3$ (10 mL), and saturated aqueous NaCl (10 mL), dried (Na_2SO_4), filtered, and concentrated. Flash chromatography (SiO_2, 90% EtOAc−hexane) provided **26** (50.3 mg, 64% overall).

[2-{N^2-BOC-N^1-(*N*-SES-D-Ser)-hydrazino}-3-(*tert*-butyldimethylsilyloxy)-4-(1,3-dioxan-2-yl)-(2*S*,3*S*)-butanoyl-Gly-Sar-L-Me-Val-(*β*-OH)]$_2$ (Serine Hydroxyl) Dilactone (28). A solution of **26** (35.5 mg, 16.3 μmol) in degassed EtOH (1.4 mL) at 25 °C was treated with 10% Pd−C (18 mg) and 25% aqueous HCO_2NH_4 (142 μL). After 4 h, additional HCO_2NH_4 (70 μL) was added, and the reaction was stirred for an additional 2 h. The mixture was filtered and concentrated. The residue was dissolved in EtOAc (30 mL) and washed with saturated aqueous NaCl (2 × 3 mL). The aqueous layer was re-extracted with EtOAc (2 × 20 mL). The combined organic phase was dried (Na_2SO_4), filtered, and concentrated in vacuo to yield **27** (32.0 mg) which was used directly in the next reaction without further purification.

A solution of EDCI (15.3 mg, 78.2 μmol) and HOAt (11.9 mg, 85.7 μmol) in CH_2Cl_2 (9.5 mL) at 0 °C was treated with a solution of **27** (32.0 mg) in CH_2Cl_2 (1.5 mL) dropwise over 1 h (25 μL/min), followed by a CH_2Cl_2 (2 × 0.5 mL) rinse dropwise over 20 min (50 μL/min). The solution was stirred at 0 °C for 16 h. The solution was diluted with CH_2Cl_2 and successively washed with H_2O and saturated aqueous $NaHCO_3$. The aqueous layer was re-extracted with EtOAc, and the combined EtOAc phase was dried (Na_2SO_4), filtered, and concentrated. Flash chromatography (SiO_2, EtOAc−hexane−CH_3CN, 5:4:1) provided **28** (19.1 mg, 63% overall).

[*N*-SES-D-Ser-L-Htp(OTBS)-Gly-Sar-L-Me-Val(*β*-OH)]$_2$ (Serine Hydroxyl) Dilactone (29). A solution of **28** (8 mg, 4.32 μmol) and anisole (120 μL) in CH_2Cl_2 (0.3 mL) at 0 °C was treated with trifluoroacetic acid (0.3 mL) and stirred for 2 h. The solution was warmed to 25 °C and stirred for an additional 1 h. The solution was concentrated, diluted with EtOAc (2.5 mL), and washed with saturated aqueous $NaHCO_3$ (2 mL). After re-extraction with EtOAc (4 × 2 mL), the combined organic phase was dried (Na_2SO_4), filtered, and concentrated. Flash chromatography (SiO_2, EtOAc−hexane−CH_3CN, 5:4:1) provided **29** (4.4 mg, 68%).

[*N*-BOC-D-Ser-L-Htp(OTBS)-GIy-Sar-L-Me-VaI(*β*-OH)]$_2$ (Serine Hydroxyl) Dilactone (31). A Teflon vessel charged with **29** (2.1 mg, 1.4 μmol) and anisole (5 drops) was treated (condensed) with 2−3 mL of anhydrous HF at −78 °C. The solution was warmed to 0 °C and stirred for an additional 75 min. The HF was removed at 0 °C under a stream of N_2 for 1 h. The residue was dissolved in H_2O, filtered, and concentrated in vacuo to provide **30** as a white residue. The residue was suspended in THF (0.5 mL), treated with $NaHCO_3$ (20 mg) and BOC_2O (10 mg), and stirred at 25 °C for 48 h. The solution was concentrated, and PLTC provided **31** (1.1 mg, 0.96 μmol, 69%).

Luzopeptin C (3). In a Teflon vessel charged with **29** (2.0 mg, 1.3 μmol) and anisole (100 μL) was condensed 2−3 mL of anhydrous HF at −78 °C. The solution was warmed to 0 °C and stirred for an additional 90 min. The HF was removed at 0 °C under a stream of N_2 for 1 h. The residue was dissolved in 1 M aqueous HCl and lyophilized to provide **30** as the HCl salt which was used directly in the next reaction.

A solution of **30** in DMF (0.30 mL) at 0 °C was treated sequentially with $NaHCO_3$ (1.3 mg, 15 μmol, 12 equiv), HOBt (1.1 mg, 7.8, μmol, 6 equiv), and 6-methoxyquinoline-2-carboxylic acid (**32**, 1.4 mg, 6.5 μmol, 5 equiv). Once the solution was homogeneous, EDCI (1.3 mg, 6.5 tmol, 5 equiv) was added. The solution was stirred at 0 °C for 1 h, warmed to 25 °C, and stirred for an additional 11 h. The solution was concentrated in vacuo. PTLC (SiO_2, 10% CH_3OH−CH_2Cl_2) provided luzopeptin C (**3**, 1.4 mg, 1.0 μmol, 80%).

Luzopeptin A (1) and Luzopeptin B (2). A solution of luzopeptin C (**3**, 2.8 mg, 2.1 μmol) in Ac_2O−pyridine (1:1, 240 μL) was stirred at 25 °C for 14 h. The solution was poured into saturated aqueous $NaHCO_3$ (6 mL), extracted with $CHCl_3$ (5 × 5 mL), dried (Na_2SO_4), filtered, and concentrated to provide the crude product (3.1 mg, 2.1 μmol, 100%) as a crude yellow solid which was used directly in the next reaction without further purification.

A solution of the product from above (3.1 mg, 2.1 μmol) in THF−CH_3OH (3:1, 0.80 mL) was treated with Na_2CO_3 (0.05 M in water, 0.20 mL) for 2 h. The solution was poured into saturated aqueous $NaHCO_3$ and extracted with $CHCl_3$ (3 × 2 mL) and CH_3CN (3 × 2 mL). The combined organic phase was dried (Na_2SO_4), filtered, and concentrated. PTLC (SiO_2, 8% CH_3OH−$CHCl_3$) provided luzopeptin A (**1**, 1.3 mg, 0.91 μmol, 48%) and luzopeptin B (**2**, 0.4 mg, 0.3 μmol, 14%).

Quinoxapeptin C (6). In a Teflon vessel charged with **29** (10.2 mg, 6.8 μmol) and anisole (100 μL) was condensed 2−3 mL of anhydrous HF at −78 °C. The solution was warmed to 0 °C and stirred for an additional 90 min. The HF was removed at 0 °C under a stream of N_2 for 1 h. The residue was dissolved in 1 M aqueous HCl and lyophilized to provide **30** as the HCl salt which was used directly in the next reaction.

A solution of **30** in DMF (1.0 mL) at 0 °C was treated with $NaHCO_3$ (8.6 mg, 102 μmol, 15 equiv), HOBt (4.6 mg, 34, μmol, 5 equiv), and 6-methoxyquinoxaline-2-carboxylic acid (**32**, 5.5 mg, 27 μmol, 4 equiv). Once the solution was homogeneous, EDCI (5.2 mg, 27 μmol, 4 equiv) was added. The solution was stirred at 0 °C for 1 h, warmed to 25 °C, and stirred for an additional 5 h. The solution was poured into saturated aqueous $NaHCO_3$ (5 mL) and extracted with EtOAc (5 × 5 mL). The combined organic phase was dried (Na_2SO_4), filtered and concentrated. PTLC (SiO_2, 8% $CH_3OH-CH_2Cl_2$) provided **6** (5.8 mg, 4.4 μmol, 65%).

Quinoxapeptin A (4). A solution of (1*S*,2*S*)-methylcyclopropanecarboxylic acid (5.6 mg, 56 μmol) in CH_2Cl_2 (40 μL) and DMF (0.0052 μmol) at 0 °C was treated with oxalyl chloride (6 μL, 67 μmol), stirred at 0 °C for 20 min, warmed to 25 °C, and stirred for an additional 1.5 h. The solution was transferred dropwise (5−10 min) by syringe to a solution of quinoxapeptin C (**6**, 1.0 mg, 0.76 μmol) in pyridine (50 μL) at 0 °C, and the resulting mixture was stirred for 1.5 h. The solution was diluted with CH_2Cl_2 (2 mL) and washed with saturated aqueous $NaHCO_3$ (2 × 2 mL) and saturated aqueous NaCl (1 × 2 mL). After re-extraction of the aqueous layer with CH_2Cl_2 (4 × 2 mL), the organic layers were combined, dried (Na_2SO_4), and concentrated. PTLC (alumina, 10 × 10 cm, 4% $CH_3OH-CH_2Cl_2$) provided **4** (0.9 mg, 0.61 μmol, 80%) and the corresponding *S*,*S*-monoester **36** (0.2 mg, 0.14 μmol, 18%).

(1*R*,2*R*)-2-Methylcyclopropanecarboxylic Acid Diester of Quinoxapeptin C (35). A solution of (1*R*,2*R*)-methylcyclopropanecarboxylic acid (8 mg, 80 μmol) in CH_2Cl_2 (40 μL) and DMF (0.0026 μmol) at 0 °C was treated with oxalyl chloride (6 μL, 67 μmol), stirred at 0 °C for 10 min, warmed to 25 °C, and stirred for an additional 2 h. The solution was transferred dropwise (5 min) by syringe to a solution of quinoxapeptin C (**6**, 0.6 mg, 0.46 μmol) in pyridine (20 μL) at 0 °C, and the resulting mixture was stirred for 1 h. The solution was diluted with CH_2Cl_2 (2 mL) and washed with saturated aqueous $NaHCO_3$ (2 × 2 mL) and saturated aqueous NaCl (1 × 2 mL). After re-extraction of the above aqueous layer with CH_2Cl_2 (4 × 2 mL), the organic layers were combined, dried (Na_2SO_4), filtered, and concentrated. PTLC (alumina, 4% $CH_3OH-CH_2Cl_2$) provided **35** (0.5 mg, 74%) and the corresponding monoester **37** (0.1 mg, 16%).

Quinoxapeptin B (5). A solution of **36** (0.4 mg, 0.76 μmol) in Ac_2O−pyridine (1:1, 480 μL) was stirred at 25 °C for 17 h. The solution was diluted with CH_2Cl_2 (3 mL), poured into saturated aqueous $NaHCO_3$ (15 mL), extracted with CH_2Cl_2 (5 × 10 mL), dried (Na_2SO_4), filtered, and concentrated. PTLC (alumina, 4% $EtOH-CH_2Cl_2$ eluent) provided **5** (0.25 mg, 0.18 μmol, 62%).

Quinoxapeptin Diacetate (38). A solution of quinoxapeptin C (**6**, 1.0 mg, 0.76 μmol) in Ac_2O−pyridine (1:1, 240 μL) was stirred at 25 °C for 15 h. The solution was diluted with CH_2Cl_2 (3 mL), poured into saturated aqueous $NaHCO_3$ (15 mL), extracted with CH_2Cl_2 (5 × 10 mL), dried (Na_2SO_4), filtered, and concentrated. PTLC (SiO_2, 6% $CH_3OH-CH_2Cl_2$) provided **38** (0.9 mg, 0.64 μmol, 84%).

DNA Binding Studies. The analogues were dissolved in DMSO to a concentration of 1 mM. A final concentration in the cuvette of 10 μM was achieved by adding 20 μL to the cuvette, diluting with DMSO to 40 μL, and then adding 1960 μL of aqueous buffer containing 10 mM Tris−HCl (pH 7.4), 75 mM NaCl. The reverse addition, of the agent to the buffer, caused significant precipitation and gave lower fluorescence intensities with a number of the agents. Type I calf thymus DNA (Sigma) was dissolved in 10 mM Tris−HCl (pH 7.4), 75 mM NaCl buffer to a concentration of 320 μM base pairs based on an extinction coefficient of 12 824 M^{-1} cm^{-1} at 260 nm. The purity was checked by assuring that the absorbance ratio at 260:280 nm was greater than 1.8. The concentration of the self-complementary deoxyoligonucleotides 5′-$(GCATGC)_2$, 5′-$(GCGCGC)_2$, 5′-$(GCTAGC)_2$, 5′-$(GCCGGC)_2$ (Genbase Inc., San Diego, CA) was established as previously described,[4] and these were diluted to 320 μM base pairs in 10 mM Tris−HCl (pH 7.4), 75 mM NaCl aqueous buffer.

The agent (20 μL, 1 mM in DMSO) was added to a clean, dry 4-mL quartz cuvette containing a Teflon-coated stirrer bar. A further 20 μL of DMSO was added, followed by 1960 μL of 10 mM Tris−HCl (pH 7.4), 75 mM NaCl aqueous buffer. After 5 min of stirring, an initial fluorescence reading was taken with minimum exposure to the excitation beam. At this point, aliquots of DNA solution (5−10 μL) were added, and the solution was allowed to equilibrate for 15 min before the subsequent readings were taken. The excitation and emission wavelengths were 360 and 530 nm for sandramycin, 340 and 520 nm for the luzopeptins, and 360 and 460 nm for the quinoxapeptins. The results of the titrations were analyzed by Scatchard analysis. For CT-DNA, the linear part of the Scatchard plot was used to determine high-affinity binding constants. For the deoxynucleotides, a nonlinear fit of the curve as described in the text was used to determine the high-affinity binding constant.

DNA Unwinding. Due to the low solubility of the agents in water, all agents were dissolved in DMSO as stock solutions, stored at −20 °C in the dark, and diluted to working concentrations in DMSO prior to addition to the DNA. A buffer solution containing 0.25 μg of supercoiled ΦX174 RF1 DNA (1.0×10^{-8} M) in 9 μL of 50 mM Tris−HCl buffer solution (pH 8.0) was treated with 1 μL of agent in DMSO. The control DNA was treated with 1 μL of DMSO. The agent-to-base pair ratios were 0.011, 0.022, 0.033, 0.044, 0.11, and 0.22 for sandramycin and 0.022, 0.033, 0.044, 0.11, and 0.22 for luzopeptin A, B, and C and quinoxapeptin A, B, and C. The reactions were incubated at 25 °C for 1 h and quenched with 4 μL of loading buffer (30% aqueous glycerol, 0.25% bromophenol blue, 0.25% xylene cyanol FF). Electrophoresis was conducted, on a 1% agarose gel at 50 V for 3 h. The gel was stained with ethidium bromide and visualized using a UV transilluminator, and the image was captured on an Eagle-Eye II (Stratagene, La Jolla, CA).

Acknowledgment. We gratefully acknowledge the financial support of the National Institutes of Health (CA41101) and the Skaggs Institute for Chemical Biology, the award of a NIH postdoctoral fellowship (F32 GM1876, M.W.L.), and the sabbatical leave of Dr. M. Kume sponsored by Shiongi Co., Ltd. (1998−1999). We also gratefully acknowledge the preparation of substantial quantities **10** by Dr. G. Schule (ref 16) and the development of the route to **16** by J.-H. Chen.

Supporting Information Available: Full characterization data on **1**−**6**, **8**, **9**, **11**−**13**, **16**−**18**, **20**, **25**, **26**, **28**, **29**, **31**, and **35**−**38**, and full details of the preparation of **33** (PDF). This material is available free of charge via the Internet at http://pubs.acs.org.

JA993019E